

# On the long-term stability of reference gases for atmospheric O<sub>2</sub>/N<sub>2</sub> and CO<sub>2</sub> measurements

By RALPH F. KEELING<sup>1\*</sup>, ANDREW C. MANNING<sup>2</sup>, WILLIAM J. PAPLAWSKY<sup>1</sup> and ADAM C. COX<sup>1</sup>, <sup>1</sup>*Scripps Institution of Oceanography, University of California, San Diego, La Jolla, CA 92093-0244, USA*; <sup>2</sup>*Formerly at Scripps Institution of Oceanography, currently at the School of Environmental Sciences, University of East Anglia, Norwich NR4 7TJ, UK*

(Manuscript received 29 March 2006; in final form 27 July 2006)

## ABSTRACT

Measurements of changes in the atmospheric O<sub>2</sub>/N<sub>2</sub> ratio have typically relied on compressed air derived from high-pressure tanks as the reference material against which atmospheric changes are assessed. The validity of this procedure is examined here in the context of the history of 18 O<sub>2</sub>/N<sub>2</sub> reference tanks compared over a 12-yr time-frame. By considering differences in tank sizes, material types, and by performing additional tests, the long-term stability of the delivered gas is evaluated with respect to surface reactions, leakage, regulator effects, and thermal diffusion and gravimetric fractionation. Results are also reported for the stability of CO<sub>2</sub> in these tanks. The results emphasize the importance of orienting tanks horizontally within a thermally insulated enclosure to reduce thermal and gravimetric fractionation of both O<sub>2</sub>/N<sub>2</sub> and CO<sub>2</sub> concentrations, and they emphasize the importance of avoiding elastomeric O-rings at the head-valve base. With the procedures documented here, the long-term drift in O<sub>2</sub>/N<sub>2</sub> appears to be zero to within approximately  $\pm 0.4$  per meg yr<sup>-1</sup>, which projects to an uncertainty of  $\pm 0.16$  Pg C yr<sup>-1</sup> (1 $\sigma$ ) in O<sub>2</sub>-based global carbon budgets.

## 1. Introduction

Precise measurements have shown that the concentration of O<sub>2</sub> in the atmosphere is decreasing slowly from year to year (Keeling and Shertz, 1992; Battle et al., 2000; Bender et al., 2005; Manning and Keeling, 2006). While too small to be environmentally significant (Broecker, 1970), the decrease is nevertheless of interest as an indicator of changes in the global carbon cycle (Keeling et al., 1993). Measurements through the decade of the 1990s, for example, showed that O<sub>2</sub> concentration decreased somewhat slower than expected from fossil-fuel burning alone, indicating that the Earth's biosphere has not been in steady state, but rather acted as a source of O<sub>2</sub> and hence also as a sink for CO<sub>2</sub> (Keeling et al., 1996; Battle et al., 2000; Manning and Keeling, 2006). Measurements of O<sub>2</sub> have proven useful, not only for diagnosing carbon sinks, but also for estimating ocean productivity (Balkanski et al., 1999; Najjar and Keeling, 2000), for constraining rates of air–sea gas exchange (Keeling et al., 1998b), and for testing ocean biogeochemistry models (Stephens et al., 1998).

The large size of the atmospheric O<sub>2</sub> reservoir makes measurements of the relatively small changes in O<sub>2</sub> concentration challenging. Resolving a land biotic sink of 2 Pg C requires the ability to detect a change of  $\sim 1.8 \times 10^{14}$  moles in the global O<sub>2</sub> abundance, which corresponds to 0.000 49% of the total burden of O<sub>2</sub> in the atmosphere. Changes in O<sub>2</sub> concentration are typically expressed in terms of the relative change in O<sub>2</sub>/N<sub>2</sub> ratio

$$\delta(\text{O}_2/\text{N}_2) = (\text{O}_2/\text{N}_2)_{\text{sample}}/(\text{O}_2/\text{N}_2)_{\text{reference}} - 1,$$

where  $\delta(\text{O}_2/\text{N}_2)$  is multiplied by 10<sup>6</sup> and expressed in ‘per meg’ units. In these units, a change of  $1.8 \times 10^{14}$  moles in the global O<sub>2</sub> abundance corresponds to a change of 4.9 per meg. In spite of the measurement challenge, there are now at least six independent O<sub>2</sub> measurement techniques in use that have demonstrated a precision at the level 6 per meg or better (Keeling, 1988a; Bender et al., 1994; Manning et al., 1999; Tohjima, 2000; Stephens et al., 2003; Stephens et al., 2006), and these methods are being variously applied for flask or *in situ* measurements by at least 12 scientific institutions.

A crucial need for all these methods, however, is calibration. The existing measurement methods are all ‘relative’ in the sense that they allow air samples to be compared to reference gases, but do not establish absolute concentrations. The need for reference gases is typically satisfied using compressed air stored in

---

\*Corresponding author.  
e-mail: rkeeling@ucsd.edu  
DOI: 10.1111/j.1600-0889.2006.00228.x

high-pressure tanks. The practice of using ‘unknown’ reference gases is sufficient for measuring changes in atmospheric  $O_2/N_2$  ratio, provided it can be demonstrated that the reference gases are sufficiently stable over time. Resolving a land sink of  $0.2 \text{ Pg C yr}^{-1}$ , for example, requires reference gases stable to  $0.5$  per meg  $\text{yr}^{-1}$ .

The use of high-pressure tanks for delivering reference gas for  $O_2/N_2$  analyses began in the 1980s (Keeling, 1988a), and the tanks used at that time have continued to be monitored on a regular basis in the atmospheric oxygen laboratory at the Scripps Institution of Oceanography, along with a growing suite of additional tanks. Considerable insight into the possible sources of instability of  $O_2/N_2$  ratios in gas tanks can be gained through a careful analysis of the long-term history of the relative composition of the air delivered from these tanks.

Following Keeling et al. (1998a), this paper provides a brief review of our measurement methods and our procedures for placing  $O_2/N_2$  data on a common scale. It expands upon Keeling et al. (1998a) by presenting the long-term record of the stability of our reference tanks in the context of possible sources of instability, including changes caused by corrosion, leakage, regulator effects, thermal fractionation, and physical adsorption of gases onto tank walls. For each of these processes, we are able to place bounds on the magnitude of any effect by examining the relative changes in tanks with different pressures, different material types, different rates of gas usage, or different sizes and configurations. We also briefly review the history of  $CO_2$  concentrations delivered from our tanks as a means to provide further insight into sources of instability that may also be relevant for both  $O_2$  and  $CO_2$  measurements. This paper includes a quantification of the uncertainties in the Scripps  $O_2/N_2$  calibration scale arising from tank instabilities which is relevant to estimate uncertainties in land and ocean carbon sinks based on the Scripps records.

## 2. Scripps reference tanks

The primary  $O_2/N_2$  reference gases (or ‘primaries’) used at Scripps consist of 12 tanks filled between 1986 and 1989, and an additional set of six filled between 1993 and 1994, as summarized in Table 1. Seven of these are 265 standard cubic foot (SCF) aluminium tanks, five are 150 SCF aluminium tanks, and six are 265 SCF chrome-molybdenum steel tanks. Six of the aluminium primaries received a proprietary inner surface treatment by Airco; all other tanks, including the steel tanks, were untreated except for routine cleaning by the supplier. The steel tanks have served as primary reference gases for our  $CO_2$  measurements, and were obtained during a period in 1989 when 265 SCF aluminium tanks were unavailable from the manufacturer (Luxfer).

All reference gases were filled using the air pumping facility at Scripps, which uses a RIX Industries pump and molecular sieves for drying. At the time of filling, the primaries had water vapour contents from  $0.7$  to  $2.2 \mu\text{mole mol}^{-1}$ , depending on the

tank. The  $O_2/N_2$  ratio of the air in these 18 tanks spans a range from  $-350$  to  $+50$  per meg on the Scripps S2 scale (see below).

## 3. Methods and Apparatus

Our methods for delivering gas from the reference tanks were described in (Keeling et al., 1998a) and have not changed since that description. A key element is the use of a thermally insulated enclosure in which the tanks are stored horizontally to minimize thermal and gravimetric fractionation. The tanks are connected to regulators located outside the enclosure using  $1/16$ -in. O.D. nickel lines, a procedure adopted primarily because it allows the pressure gauges on the regulators to be read without opening the enclosure, although it also has merit in separating the regulator from the tank itself.

The delivery of air from the tanks involves the following steps: (1) the high-pressure lines are pressurized and vented at least three times before they are left open to the tank, (2) the high-pressure lines are left open to the tank for at least 2 h, and (3) the high-pressure lines, still at tank pressure, are swept out at a flow of  $5 \text{ STP cm}^3 \text{ s}^{-1}$  for  $\sim 10$  min to minimize artefacts associated with conditioning the regulators and high-pressure lines connecting the tank and regulator. In addition, we require that the tanks be stored horizontally in the enclosure for at least 10 hours prior to analysis. These 10 h necessarily overlap with steps (2) and (3) above. During analysis, we deliver gases at  $\sim 5 \text{ STP cm}^3 \text{ s}^{-1}$ . Tanks are typically analysed on a repeated basis (10 min ‘on’, 10 min ‘off’), alternating with other tanks or flasks. During such cycling, a lower flow of  $0.8 \text{ STP cm}^3 \text{ s}^{-1}$  is maintained, even during the ‘off’ mode, to reduce artefacts associated with preferential permeation of  $O_2$  and  $CO_2$  through O-rings in the regulators.

Our laboratory is equipped with an interferometric  $O_2$  analyser (Keeling et al., 1998a; Keeling, 1988b), a Siemens Ultramat 3  $CO_2$  analyser, and an ISOPRIME mass spectrometer system that analyses  $O_2/N_2$ ,  $Ar/N_2$ , and  $CO_2/N_2$  ratios (Keeling et al., 2004). The interferometric and Ultramat analysers have been in use since 1986, and the mass spectrometer since June 2001.

## 4. Calibration Scale Development

The primary reference gases serve to provide a stable  $O_2/N_2$  reference on time-scales of six months and longer. On shorter time-scales, we rely on an independent set of shorter-lived tanks consisting of ‘working tanks’ and ‘secondaries’. At any given time, one working tank and two secondaries are in service. The working tank is used to establish the instrument baseline against which all other gases, including primaries, secondaries, and flask samples, are analysed. Working tank flow is essentially continuous during analysis, which causes the working tanks to be exhausted on a time-scale of a few months. The working tank concentration is assigned based on a daily calibration against the secondaries, thus correcting for any drift in the working tank

Table 1. Reference tank characteristics

Tank ID #	Manufacturer <sup>a</sup>	Cyl. Mat. <sup>b</sup>	Dimensional internal Volume (l)	Capacity (SCF) <sup>c</sup>	Surface <sup>d</sup>	Valve <sup>e</sup>	Valve connection	Dip-tube	Fill date	Leakage	Pressure (MPa)		
											January 1990	January 1996	January 2002
CC43230	L	Al	29	150	SP	B	Pipe	no	December 85	No	10.4	9.8	8.7
CC43418	L	Al	29	150	SP	B	Pipe	no	December 85	No	9.8	9.1	7.8
HA5178	L	Al	47	265	SP	SS	Pipe	no	September 86	Yes	9.8	8.0	5.6
HA6999	L	Al	47	265	SP	SS	Pipe	no	September 86	No	12.5	11.8	11.1
HA7014	L	Al	47	265	SP	SS	Pipe	no	September 86	No	4.9	4.0	3.7
HA7017	L	Al	47	265	SP	SS	Pipe	no	September 86	Yes	8.4	5.3	4.2
635862	TW	S	49	300		SS	Pipe	no	January 90	Yes	16.0	14.6	13.2
635864	TW	S	49	300		SS	Pipe	no	January 90	No	16.0	14.9	13.5
635866	TW	S	49	300		SS	Pipe	no	January 90	Yes	17.3	11.8	10.6
635867	TW	S	49	300		SS	Pipe	no	November 89	No	16.0	13.9	12.5
635868	TW	S	49	300		SS	Pipe	no	January 90	No	16.7	14.6	13.5
635870	TW	S	49	300		SS	Pipe	no	January 90	No	16.7	15.3	12.9
CC105762	L	Al	29	150		B	Flange	yes	August 94	No		11.8	10.9
CC106697	L	Al	29	150		B	Pipe	yes	August 94	No		12.0	10.9
CC106703	L	Al	29	150		B	Pipe	yes	August 94	No		13.2	11.8
ND01598	L	Al	46	265		B	Flange	yes	December 93	No		11.3	10.3
ND02698	L	Al	46	265		B	Pipe	no	January 95	No		14.2	13.2
ND02705	L	Al	46	265		B	Pipe	yes	July 94	No		14.2	13.5

<sup>a</sup>Luxfur (L); Taylor–Wharton (TW).<sup>b</sup>Aluminium (Al); chrome-molybdenum steel (S).<sup>c</sup>Rated fill capacity in standard cubic feet (SCF). 1 SCF = 28.32 STP l.<sup>d</sup>Spectra-seal (SP); a blank denotes no treatment other than standard cleaning. Spectra-seal is a proprietary treatment provided by Airco.<sup>e</sup>Brass (B); Stainless-Steel (SS). All our tanks valves have PCTFE seats. The valves were supplied either by Ceodeux (tanks filled after Jan 1994) or by Superior Valve Company (all other tanks).<sup>f</sup>Valves connected with pipe thread were sealed with standard Teflon tape. Valves connected with flanges were sealed with a spring-loaded, silver-coated, stainless-steel ‘C’ ring, manufactured by Helicoflex.

on time-scales longer than 1 d. The daily calibration adopts an assigned (fixed) value for each secondary, as discussed below, and typically assumes a linear instrument response.

The secondaries also have a fairly short lifetime of  $\sim 2$  yr, and replacements are staggered so that only one of the two secondaries is replaced at any given point in time. A replacement first involves making repeated comparisons with the existing secondaries, to establish the assigned concentration of the new tank. The sequence of secondary gases forms the basis of a preliminary scale, known as the 'S1' scale, that can be propagated forwards in time indefinitely, but which may drift slowly in absolute terms due to either instabilities in the secondary gases or random errors in their initial assigned concentrations. To eliminate this drift, we apply a drift correction function of the form  $S2 = S1 + C(t)$ , where S2 is the value on the corrected scale, and  $C(t)$  is a time-varying function. The drift correction function is assessed primarily based on repeated analyses of the primaries, which for this purpose are typically assumed to have been sta-

ble. The validity of this assumption can only be established by additional consistency checks, as discussed below. As new information becomes available, the drift correction function is subject to retrospective revision, with each revision yielding a slightly different version of the S2 scale.

Figure 1 shows the time-histories of the primaries on the S2 scale (2 June 2003 revision) as well as the drift correction function  $C(t)$  relating the S2 and S1 scales. To emphasize small time-dependent anomalies, a time-invariant offset has been subtracted from each tank before plotting. Several features are notable. First, the drift correction function is virtually flat after mid-1991, ranging only between  $+5$  and  $+10$  per meg. Secondly, the primaries have also generally remained highly stable on the S2 scale, at least since late 1992. A clear implication is that both the primaries and the secondaries have remained quite stable in relative terms since late 1992.

Thirdly, an upward shift in the aluminium primaries is notable in 1992 which we have not minimized using the drift correction

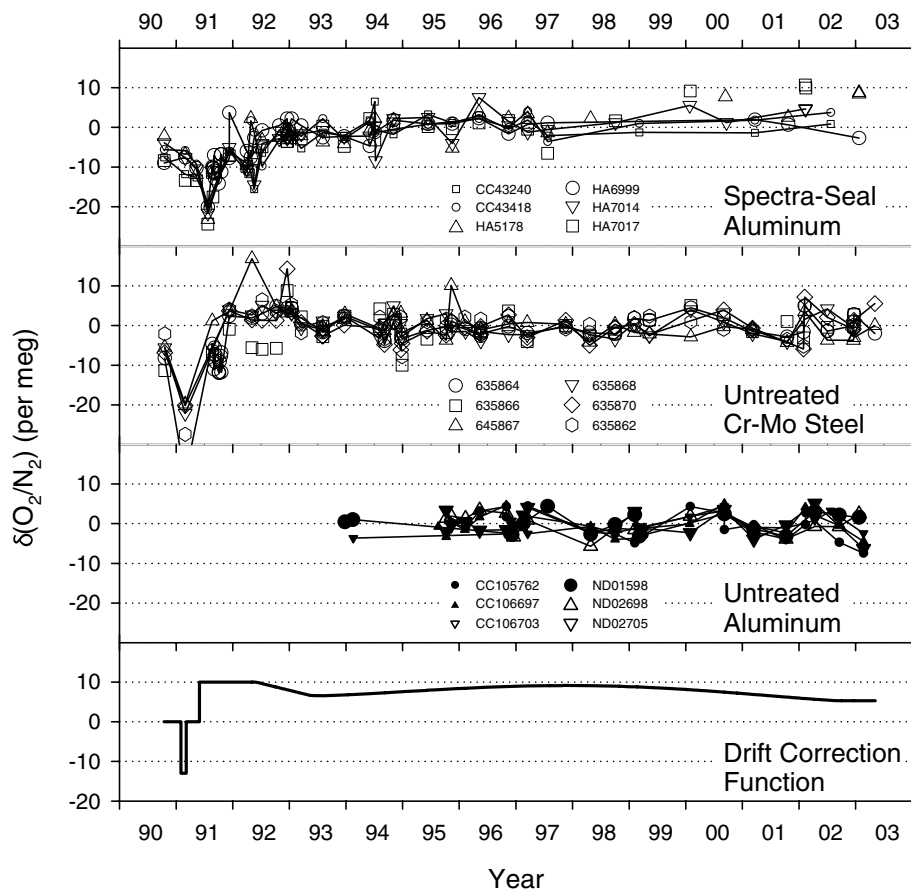


Fig. 1.  $O_2/N_2$  ratios (S2 scale) of primary reference tanks sorted by tank material type (top three panels) and the drift correction function (bottom panel) which has been applied to all tanks (converts S1 to S2 values, see the text). For each tank, the mean value since October 1992 has been subtracted, thus showing only the residuals from this tank mean. Small symbols: 150 SCF tanks; large symbols: 265 SCF tanks. Solid symbols: tanks with dip tubes; hollow symbols: tanks without dip tubes. Lines connect points for an individual tank. Tanks that are known to have leaked are shown without connecting lines.

function. We have not minimized this shift because we have established, based on prior work (Keeling et al., 1998a), that it corresponds to an actual change in the composition of the air delivered from the aluminium primaries when they were moved from an upright position in the laboratory to a horizontal position in the enclosure. We have not eliminated certain additional shifts in the primaries before 1992 which we also expect reflect real thermal-induced changes in the delivered gas concentrations prior to the time when the tanks were moved into the enclosure, as discussed in Keeling et al. (1998a). After mid-1992, the standard deviation of the individual daily tank determinations on the S2 scale is around  $\pm 2.8$  per meg.

Fourthly, at least two of the primaries show slight upwards drift relative to the other primaries. By 2003 this drift had become a concern. We then inspected all our primary tanks for leaks using a liquid leak detector (Snoop®) and discovered that the drifting tanks were leaking through faulty seals at the burst discs of the head valves. The inspection also identified two additional tanks that were leaking but were not previously flagged based on drift. Based on the tank pressure histories, we verified that the leakage had occurred steadily for years. Since they are known to have been faulty, we exclude all leaking tanks from subsequent analyses [e.g. constructing  $C(t)$ ].

## 5. Constraints on absolute $O_2/N_2$ stability

The records show that our primaries have maintained a high degree of stability relative to each other over the duration of our programme. The secondaries have also maintained high stability relative to the primaries. High relative stability presumably places constraints on the absolute stability of the tanks, but how strong are these constraints? To answer this question, we consider a range of possible drift mechanisms, and use experimental constraints to place bounds on their magnitude.

### 5.1. Corrosion and long-term surface reactions

One possible drift mechanism involves the consumption of  $O_2$  by slow oxidative corrosion of the inner walls of the tank or other long-term surface reactions. If long-term surface reactions were important, we would expect this to impact tanks differently depending on the inner surface type. To examine if surface type influences tank stability, we have grouped the tank data (shown in Fig. 1) by tank material type and we have fit linear trends (not shown in the figure) through the grouped results to infer linear drift rates, as summarized in Table 2. Because several of the untreated aluminium tanks were not brought into use until 1995, we report rates over two periods: (1) from August 1992 to April 2003, allowing steel and treated aluminium tanks to be compared, and (2) from January 1995 to April 2003, allowing all three types to be compared.

Focusing on results from the 1/95–4/03 period, we find no evidence of systematic drift in any tank type on the S2 scale, and

Table 2. Summary of tank drift in per meg  $yr^{-1}$  (relative to S2 scale)

Tank type	Time period		
	8/92–4/03	8/92–1/95	1/95–4/03
<i>By material</i>			
Aluminium, treated*	$0.34 \pm 0.10$	$0.41 \pm 0.53$	$0.07 \pm 0.16$
Steel	$-0.13 \pm 0.08$	$-1.89 \pm 0.48$	$0.08 \pm 0.11$
Aluminium, untreated			$-0.09 \pm 0.11$
<i>By size</i>			
150 SCF tanks	$0.05 \pm 0.09$	$1.06 \pm 0.72$	$-0.12 \pm 0.12$
All other tanks	$-0.05 \pm 0.06$	$-1.56 \pm 0.48$	$0.00 \pm 0.09$

\*

the relative drift between tank types is also small: the relative drift between the treated aluminium and steel tanks is estimated at  $0.01 \pm 0.19$  per meg  $yr^{-1}$ , while that between untreated aluminium tanks and the steel tanks is  $-0.17 \pm 0.16$  per meg  $yr^{-1}$ .

To translate these constraints on relative drift into a constraint on absolute drift, we must make an assumption about the degree to which the absolute drift rates of the different tank types might be matched with one another. It is helpful here to introduce the concept of a ‘matching factor’, which measures relative drift rate of two tank types. A matching factor of 1.0 implies that the two types are drifting at exactly the same rate, while a factor of 10 implies that one type is drifting at a rate 10 times higher or lower than the other.

As an example, we first assume that the matching factor between any pair of tank types is at best 2. In other words, if one tank type is drifting at rate  $X$ , then the other tank types are considered unlikely to be drifting at rates between  $0.5X$  and  $2X$ , but rather to be drifting at rates outside this range. Scenarios can then be constructed that are consistent both with the bounds on relative drift from the fits and this constraint on the matching factor. By trial and error, we find a worst-case scenario in which the untreated aluminium tanks are drifting by  $-0.3$  to  $-0.4$  per meg  $yr^{-1}$  and the remaining tanks are drifting at rates between  $-0.1$  to  $-0.2$  per meg  $yr^{-1}$ . In this worst-case scenario, the S2 scale drifts (undetectably) at a rate of  $0.1$  to  $0.3$  per meg  $yr^{-1}$ . The constraints are also compatible, of course, with a best-case scenario in which the drift in the S2 scale is zero.

Scenarios that allow for greater drift in the S2 scale are possible if we assume the matching factor is not 2, but rather 1.5, etc. However, there are clearly bounds on what is reasonable. For example, it seems improbable that tanks with very different surface types would lose oxygen at rates that were matched to within 10% (matching factor = 1.1), but not remarkable if rates were matched to within a factor of 10. The factor of 2 is near the low end of the reasonable range.

Although we see little evidence of relative drift over the long term, a detectable downward drift in the steel tanks relative to the aluminium tanks of  $\sim 5$  per meg is notable over a specific period

from 8/92 to 1/95. The drift is evident visually in Fig. 1 and is reflected in the fitted trends in Table 2. If the 8/92–1/95 trend were caused by oxidation, we would expect an even steeper drift rate before 8/92, consistent with a reaction that proceeds most rapidly near the beginning of the tank history and reduced as the tank walls are slowly conditioned. The data, however, do not show such an effect, thus probably ruling out oxidation as the cause of the 8/92–1/95 relative drift. We do not fully understand the origin of this drift, but suspect that it may reflect differences in thermal fractionation of steel and aluminium tanks, as discussed below.

In summary, we see no evidence of detectable corrosion effects on our tanks at any point in their history. Any systematic effect appears to be less than 0.3 per meg  $\text{yr}^{-1}$  over the long term.

## 5.2. Leakage and Permeation

The composition of tank air can potentially be influenced by leakage through small orifices or by permeation through elastomeric seals or seats in the head valves. Our primaries have several different head valve types, some joined to the tank with pipe fittings sealed with Teflon tape, and some sealed with metallic C-rings (see Table 1). All the head valves used have seats made from poly-chloro-tri-fluoro-ethylene (PCTFE), a material with low but non-zero permeability to gases (Sturm et al., 2004).

Because  $\text{N}_2$  has a higher kinetic velocity than  $\text{O}_2$ , orifice leakage will enrich the  $\text{O}_2/\text{N}_2$  ratio in the tank. Just such an effect was observed for our leaking tanks, described above. In contrast, permeation loss will cause tanks to become depleted in  $\text{O}_2$  relative to  $\text{N}_2$  because  $\text{O}_2$  has higher permeability than  $\text{N}_2$  through most elastomers, including PCTFE (Sturm et al., 2004). A downward drift in  $\text{O}_2/\text{N}_2$  ratio has been observed in pressurized glass flasks with elastomeric seals on the stopcocks (Sturm et al., 2004), as well as in high-pressure tanks employing elastomeric O-ring seals at the valve base, as described below.

We have directly measured the permeation rate of gases through the valve seats using a test set-up in which a tank head valve (Ceodeux) was connected to a mock-up of a tank head connection that allowed the high-pressure side of the valve to be alternately evacuated or pressurized without opening the valve. The low-pressure side of the head valve was connected to a small ( $5.4 \text{ cm}^3$ ) test volume that could be evacuated and sealed. The absolute pressure in this test volume was measured using a sensitive differential pressure gage (MKS Model 223B,  $\pm 1$  torr) that was connected on the reference side to a vacuum maintained with a rotary vane pump. The test sequence involved first evacuating both sides of the valve, sealing the test volume for a period of time, and then pressurizing the high-pressure side. The head valve was closed throughout this sequence. The closing torque of the head valve was not controlled – it was just closed as in a normal operating situation. Permeation through the valve seat was assessed from the change in the leak-up rate in the test volume following pressurization. The sequence was repeated for

different periods of time with several different gas types (pure He, Ar,  $\text{N}_2$ , and natural air) in order to assess species-specific permeation rates.

The background leak-up/outgassing rate of the volume, measured with the high-pressure side of the valve evacuated, was  $\sim 6.0 \times 10^{-10} \text{ STP cm}^3 \text{ s}^{-1}$ . Following pressurization with He at 15.4 MPa (154 atm), an enhanced leak-up rate of  $8.5 \times 10^{-7} \text{ STP cm}^3 \text{ s}^{-1}$  was observed, which we attribute to permeation through the valve seat. For all other gases, the enhancement following pressurization (Ar at 15.1 MPa,  $\text{N}_2$  at 15.3 MPa, Air at 13.2 MPa) was too small to be detected. In the case of air, runs as long as 551 h were conducted to allow for the possibility that the ‘breakthrough’ due to permeation was very slow. However, even for such long runs, no detectable increase in leak-up was noted.

The results for air allow bounds to be placed on the maximum drift rate of  $\text{O}_2/\text{N}_2$  in tanks due to valve-seat permeation. Pessimistically adopting a detection threshold of  $6.0 \times 10^{-10} \text{ STP cm}^3 \text{ s}^{-1}$  and applying this to a 150 SCF tank at 13.2 MPa, the tank drift is bounded between  $-0.02$  and  $0.006$  per meg  $\text{yr}^{-1}$ , depending on whether the permeation is assumed to be dominated by  $\text{O}_2$  (low bound) or  $\text{N}_2$  (high bound). These results show that permeation through the valve seat is too small to be significant.

To constrain the effects of permeation through other seals (e.g. valve base, diaphragm & burst disk seals) or due to leakage through orifices, we rely on the fact that any such process, if systematically influencing our tanks, would influence smaller tanks more than larger tanks. Specifically, if permeation were uniformly influencing our tanks, it would cause the  $\text{O}_2/\text{N}_2$  ratio of our smaller tanks to drift slowly downwards relative to our larger tanks, whereas if orifice leakage were uniformly influencing our tanks, it would cause the  $\text{O}_2/\text{N}_2$  ratio of our smaller tanks to drift slowly upwards relative to our larger tanks.

From the results summarized in Table 2, the differential drift rate of the smaller (150 SCF) tanks relative to the larger (265 or 300 SCF) tanks over the longest period (8/92–4/03) is estimated at  $0.09 \pm 0.11$  per meg  $\text{yr}^{-1}$ , a result which is not significantly different from zero but more consistent with a small orifice effect than with a permeation effect. Assuming the differential drift resulted from absolute drift that is inversely proportional to tank’s dimensional internal volume (Table 1), the differential drift of  $0.09 \pm 0.11$  per meg  $\text{yr}^{-1}$  implies absolute drift rates of  $0.23 \pm 0.27$  per meg  $\text{yr}^{-1}$  for our smaller tanks and  $0.14 \pm 0.17$  per meg  $\text{yr}^{-1}$  for our larger tanks. Based on these results and the distribution of small and large tanks in our full ensemble of primaries, we estimate that any effect of permeation or leakage on our S2 scale is bounded at the level of  $\pm 0.2$  per meg  $\text{yr}^{-1}$ .

The data in Table 2 also indicate a possibly significant trend with tank size over the shorter period 8/92–1/95. The origin of this trend is unclear, but the lack of a size-dependent trend over the longer period 8/92–4/03, discussed earlier, is probably sufficient to rule out significant leakage or permeation effects more generally.

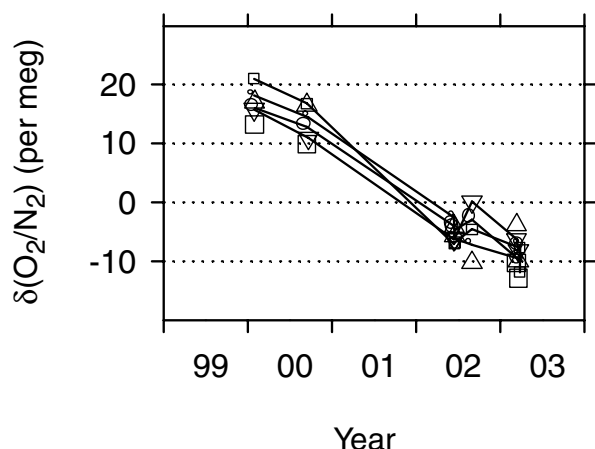


Fig. 2.  $O_2/N_2$  ratios (S2 scale) of a set of six tanks (distinct from the primaries). These tanks were untreated aluminium 150 SCF Luxfer tanks with a brass head valve (no dip tube), that used Viton, rather than Metal C-rings at the valve base. The significant downward drift in these tanks is a consequence of preferential permeation of  $O_2$  through the Viton O-rings.

As a cautionary note, we present results for a set of six tanks (not part of our primary reference gas suite) that employed Viton® fluoroelastomer O-rings as opposed to metallic C-rings or Teflon tape at the head valve base, as shown in Fig. 2. The configuration of these tanks was essentially identical to our aluminium primaries except for these O-rings. These tanks all show a persistent decrease in  $O_2/N_2$  with time of approximately  $-8$  per meg  $yr^{-1}$ , consistent with preferential permeation of  $O_2$  through the O-ring. Curiously, several additional tanks (not shown) valved at a different time in our laboratory with Viton O-rings show considerably lower though possibly still significant downward drift in  $O_2/N_2$ . The different drift rates might plausibly be caused by differences in the type of Viton®. In any case, our results show that valves configured with elastomeric O-rings, as they are often supplied by the manufacturer, may be problematic for use as long-term  $O_2/N_2$  reference gases.

### 5.3. Regulator Effects

We have exclusively used Model 14 regulators from Scott Specialty Gases (equivalent to Model 1002 from Air Liquide). One limitation with these regulators is that the first stage uses a piston with a sliding O-ring seal, which presents a virtual leak path (via permeation) to ambient pressure. We have shown, however, that by maintaining sufficient flow (as described above), we achieve consistency in the delivered gas to the level of 1 per meg. This was demonstrated by connecting multiple regulators to one tank and verifying that gas of the same composition was delivered through both regulators (Keeling et al., 1998a).

It may be of some interest to report that we have seen no evidence for fractionation of  $O_2/N_2$  due to orifice effects in the reg-

ulators, nor does such an effect seem possible under steady-state conditions. As gas flows through a tank outlet, there is a 'point of no return', located at a distance  $L$  downstream of the outlet, where molecules can no longer propagate upstream via turbulent or molecular diffusion and return to the tank. A regulator orifice located downstream of the point of no return cannot influence the composition of the delivered gas because all molecules that reach the orifice are unavoidably swept downstream by the bulk flow. For laminar flow (appropriate for our flow conditions),  $L$  is roughly equal to (or at most several times larger than) the length-scale  $DP \pi r^2 / q$ , where  $D$  is the diffusivity of  $O_2$  in air,  $q$  is the volume flow,  $r$  is the inner radius of the line, and  $P$  is the tank pressure. For our lab conditions, we have  $q = 5 \text{ atm cm}^3 \text{ s}^{-1}$ ,  $r = 0.2 \text{ cm}$ , and  $DP = 0.2 \text{ cm}^2 \text{ s}^{-1} \text{ atm}$  (Reid et al., 1987), which yields  $L \approx 5 \times 10^{-3} \text{ cm}$ . The small value of  $L$  indicates that the point of no return is effectively the tank outlet itself, which is obviously upstream of any regulator orifice. (Note that  $DP$  is effectively independent of pressure because  $D$  is nearly proportional to  $1/P$ .)

The influence of the regulator is restricted to a small region upstream of the regulator, where the concentration will vary according to  $C(x) = C_0 - \Delta C e^{-x/L'}$ , where  $x$  is the distance away from the regulator in the upstream direction,  $C_0$  is the original concentration exiting the tank,  $\Delta C$  is the regulator fractionation, and  $L'$  is the same as  $L$ , except defined for the geometry immediately upstream of the regulator orifice. Downstream of the regulator, the concentration is restored to  $C_0$ , as follows from consideration of mass balance.

These considerations do not rule out the possibly of significant regulator fractionation under non-steady conditions when flow is first established. Non-steady-state fractionation is not relevant in our laboratory, however, given the relatively high flow rates and long conditioning times employed, but it might become relevant in laboratories attempting to deliver much smaller quantities of gas.

### 5.4. Thermal and gravimetric fractionation

Compressed air tanks are potentially influenced by both gravimetric fractionation and thermal diffusion. In barometric equilibrium,  $O_2/N_2$  ratios will decrease by 17 per meg per meter of height, an effect which can be reinforced by thermal diffusion via the tendency of  $O_2$  to concentrate in colder regions and the tendency of warmer gas to collect above colder gas. Gravimetric effects are potentially counteracted by convective overturning within the tank, and thermal effects may be similarly counteracted, although probably less effectively because the temperature differences that drive convection will also tend to drive thermal separation.

Based on evidence that some combination of thermal and gravimetric fractionation was occurring in our primary tanks, we took the precaution in 1992 of laying our primaries on their sides within a thermally insulated enclosure. We expected that this

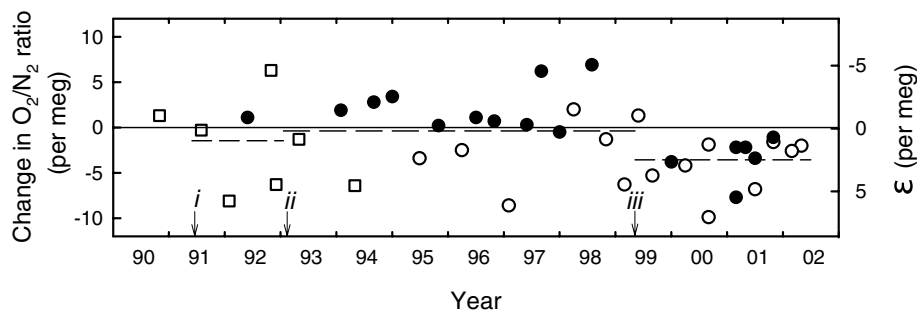


Fig. 3. Change in  $O_2/N_2$  ratio delivered from working tanks as a function of time. The left axis shows the change in  $O_2/N_2$  ratio between the full tank and the tank with 25% of the air remaining; the right axis shows the corresponding fractionation factor (see the text). Each working tank is denoted by a single point, plotted at the central time when the tank was in use. Solid circles: aluminium tanks with dip-tubes; hollow circles: aluminium tanks without dip-tubes; hollow squares: steel tanks without dip-tubes. The dashed lines denote time-averages over periods bounded by specific events: (i) working tanks and secondaries moved into the insulated enclosure, (ii) first laboratory move, and (iii) second laboratory move.

step would essentially completely eliminate gravimetric fractionation, since the air would then be withdrawn from the vertical mid-point, where the gravimetric fractionation would be zero relative to the tank average. This step should also similarly reduce the effects of thermal fractionation driven by vertical temperature gradients.

Thermal fractionation caused by horizontal temperature gradients might still be important, however. For example, if the tank outlet were warmer or cooler than the gas immediately upstream in the tank, this could lead to a slight preference for  $N_2$  or  $O_2$  to enter the outlet. This effect could potentially influence all our tanks similarly, given that the tanks are mounted with a similar orientation and thus exposed to similar temperature gradients within the enclosure. Although we cannot measure the temperature gradient between the tank outlet and the gas immediately upstream, we have measured temperature differences from one end of the tanks to the other in the enclosure. While early spot checks suggested end-to-end differences of  $0.02^\circ\text{C}$  or smaller (Keeling et al., 2004), more recent investigations have shown differences as large as  $0.3^\circ\text{C}$ . The relevant thermal diffusion coefficients are unknown at high pressures, but at 1 atm, a gradient of  $0.3^\circ\text{C}$ , could lead to 18 per meg differences in  $O_2/N_2$  due to thermal diffusion (Keeling et al., 1998a). Although the gradients near the tank outlet are presumably much smaller than  $0.3^\circ\text{C}$ , a significant thermal diffusion effect is not easily excluded based on the characteristics of our thermal enclosure.

If thermal fractionation at the tank outlet were important, we would expect to see differences between tanks equipped with 'dip tubes' and tanks without dip-tubes. The dip-tubes force the withdrawn air to come from deeper in the tank, where thermal gradients are presumably smaller. Five of our primary tanks are equipped with such tubes, with lengths varying between 15 and 23 cm. From Fig. 1, it seems possible that these tanks have exhibited slight upward and downward excursions relative to the other tanks, but the effects are bounded at the level of  $\pm 3$  per meg ( $1\sigma$ ) on a short-term basis and the level of  $\pm 1$  per meg when

averaged over yearly time-scales. A reasonable interpretation might be that the tanks with dip tubes remained more stable while the others drifted up or down.

Another constraint on thermal fractionation can be developed based on mass balance. If the air withdrawn from a tank is altered by fractionation at the outlet, there must be a reciprocal effect on the air remaining in the tank, with the effects accumulating as the tank is progressively depleted, as for a Rayleigh-type distillation. Our best means to detect such an effect is via our working tanks, which are used at the same flow rates and stored in same enclosure as the primaries, but which are depleted more rapidly. The drift in the  $O_2/N_2$  ratio of the gas delivered from each of our working tanks since the initiation of our programme is shown in Fig. 3. Each working tank is denoted by a single point, plotted at the mid-point of the time-interval when the tank was in use. The drift was computed as the difference in  $O_2/N_2$  ratio between the full tank ( $\sim 14$  MPa) and the tank at the point when 25% of the original gas remained ( $\sim 3.5$  MPa).

According to the Rayleigh model, the working-tank drift values in Fig. 3 can be converted into a fractionation factor  $\epsilon$  by dividing by  $\ln(0.25)$ , where 0.25 is the fraction of the tank air remaining at the defined end-point. Here  $\epsilon$  measures the difference in per meg units between air withdrawn from the tank and the remaining air. The estimates of  $\epsilon$ , shown in the right axis of Fig. 3 exhibit a mean of 1.1 per meg, a standard deviation of  $\pm 3$  per meg, and a range from  $-5$  to  $+7$  per meg. While these estimates of the outlet fractionation factor  $\epsilon$  were derived from working tanks alone, they are presumably also applicable to other tanks in the enclosure, given that all tanks are used at the same flow rates and are exposed to similar temperature gradients.

Our laboratory has been located in three different buildings, with moves in January 1993 and April 1999. An important question is whether differences in the thermal environment of the buildings caused systematic shifts in the air delivered from our primaries from one laboratory to the next. From the results in Fig. 3, we estimate that the mean and standard error of  $\epsilon$  for the



three buildings, in consecutive order, are  $1.0 \pm 2.1$ ,  $0.2 \pm 0.7$  and  $2.6 \pm 0.6$  per meg, with the change from the second to third building being apparently significant. In the first and third buildings, there were no significant difference between working tanks with and without dip tubes, while in the second building there were significant differences: mean and standard error of tanks with and without dip tubes are  $2.1 \pm 0.8$  and  $-3.5 \pm 1.2$  per meg, respectively. The results also show possibly larger variations in  $\varepsilon$  for the steel working tanks, which were used before April 1994, versus aluminium tanks (with or without dip tubes), which were used both before and after April 1994. Larger variability for steel tanks is not unexpected, because steel has a thermal conductivity several times smaller than aluminium, which will cause steel tanks to be generally less uniform in temperature than aluminium tanks. Surface effects are also probably more pronounced with steel tanks.

Since 2001 we have also measured Ar/N<sub>2</sub> concentrations in the working tanks and have shown that the Ar/N<sub>2</sub> ratio drifts in parallel with O<sub>2</sub>/N<sub>2</sub>. The changes in Ar/N<sub>2</sub> are around 2.5 times larger than those for O<sub>2</sub>/N<sub>2</sub>, which is consistent with the relative effect expected for thermal fractionation (Keeling et al., 2004).

Figure 3 indicates that  $\varepsilon$  may have varied, not only systematically for different configurations of our laboratory, but also quasi-randomly on shorter time-scales. The possibility of shorter-term variability in fractionation was also suggested by comparing the history of tanks with and without dip-tubes (shown in Fig. 1). The results from Figs. 1 and 3 are consistent in indicating that tanks without dip tubes exhibit short-term variability of the order of  $\sim \pm 3$  per meg, and that tanks with dip tubes likely exhibit less variability. This variability presumably applies on time-scales of hours to months, with smaller effects on annual averages.

In summary, the procedure of storing tanks horizontally within an insulated enclosure appears to be able to reduce thermal fluctuations in the O<sub>2</sub>/N<sub>2</sub> ratio delivered from gas tanks to the level of  $\pm 3$  per meg on short time-scales and probably lower levels of around  $\pm 2$  per meg on annual or longer time-scales. Our experiences before 1992 make it clear that this level of stability would not be achievable if our tanks had remained upright in the laboratory. It seems possible that the residual variability is still caused by thermal fluctuations and could therefore be reduced with improved thermal isolation.

### 5.5. Desorption effects

As the pressure in a tank decreases through usage, the O<sub>2</sub>/N<sub>2</sub> ratio of the air in the tank has the potential to be altered as gases adsorbed onto the inner walls of the tank are released into the gas phase. We can put bounds on the magnitude of any such effect using the same working tank data which we used above to constrain thermal fractionation effects (Fig. 3). The percent depletion of our primary tanks ranges from 5 to 25% from 1990 to 2002, excluding those tanks which leaked. Since the mean drift rate of our working tanks was no larger than a few per meg

over a 75% pressure drop, the working tank drift translates to a maximum desorption effect in our primaries, since they were brought into use, of 1 per meg, or less than 0.1 per meg yr<sup>-1</sup>.

## 6. CO<sub>2</sub> stability in tanks

To provide additional insight into sources of instability in reference tanks, we briefly report results for CO<sub>2</sub> concentration, which we have also routinely analysed in our reference gases, and which may be of some general interest. Our CO<sub>2</sub> results are reported on an internal CO<sub>2</sub> scale (Keeling et al., 1998a) which is closely tied to the absolute manometric CO<sub>2</sub> scale maintained in the laboratory of C.D. Keeling (also at the Scripps Institution of Oceanography). Because the link to the manometric scale is not as precise as our internal tank comparisons, however, we focus here only on relative trends between tanks, as can be resolved in our laboratory alone.

Figure 4 shows the CO<sub>2</sub> histories of our primary reference tanks on our internal CO<sub>2</sub> scale. We excluded two of the steel tanks from consideration because they have CO<sub>2</sub> concentrations too high or too low to be measured precisely in our lab. As in Fig. 1, we have subtracted a time-invariant offset from each tank before plotting. Aside from a few obvious outliers, the variations are mostly within  $\pm 0.1$  ppm. Tank leakage does not appear to have influenced CO<sub>2</sub> systematically (in contrast to O<sub>2</sub>/N<sub>2</sub>). Tank size and configuration (e.g. dip tube) also seem to have no effect on CO<sub>2</sub> stability.

Small trends are nevertheless notable based on material type. From late 1993 to 2003, the aluminium tanks (both treated and untreated) drifted detectably downwards by around  $-0.008 \mu\text{mol mol}^{-1} \text{ yr}^{-1}$ , relative to the steel tanks, and even more rapid drift in the same direction as is evident before 1993. A reasonable explanation is that the drift was caused by ‘conditioning’ wall reactions that took place in the steel tanks in the first few years after they were filled (see Table 1 for fill dates), and a simple explanation for the slower drift after 1993 is that such reactions continued beyond the first few years, but at a slower rate. Because our internal scale is anchored to our steel tanks, this would imply that our scale has drifted by 0.1–0.2 ppm over the time-frame shown. Whatever is causing this CO<sub>2</sub> drift, it appears to have had no detectable impact on O<sub>2</sub>/N<sub>2</sub> ratios. It seems likely that the drift is caused by surface reactions involving CO<sub>2</sub> but not O<sub>2</sub> and N<sub>2</sub>.

In many laboratories, a tendency has been noted for the CO<sub>2</sub> concentration delivered from compressed air tanks to drift upwards with tank usage. The drift over the lifetime of a tank is typically at least  $0.05 \mu\text{mol mol}^{-1}$ , but can also be several times larger than this (CD Keeling and Pieter Tans, personal communication). Recently, it has been shown that drift of this sort can be caused by fractionation associated with withdrawing air from tanks (Langenfels, 2002), which leads to a Raleigh-type enrichment of the remaining air, as discussed above for O<sub>2</sub>/N<sub>2</sub> ratios. Drift in the upward direction is consistent with some

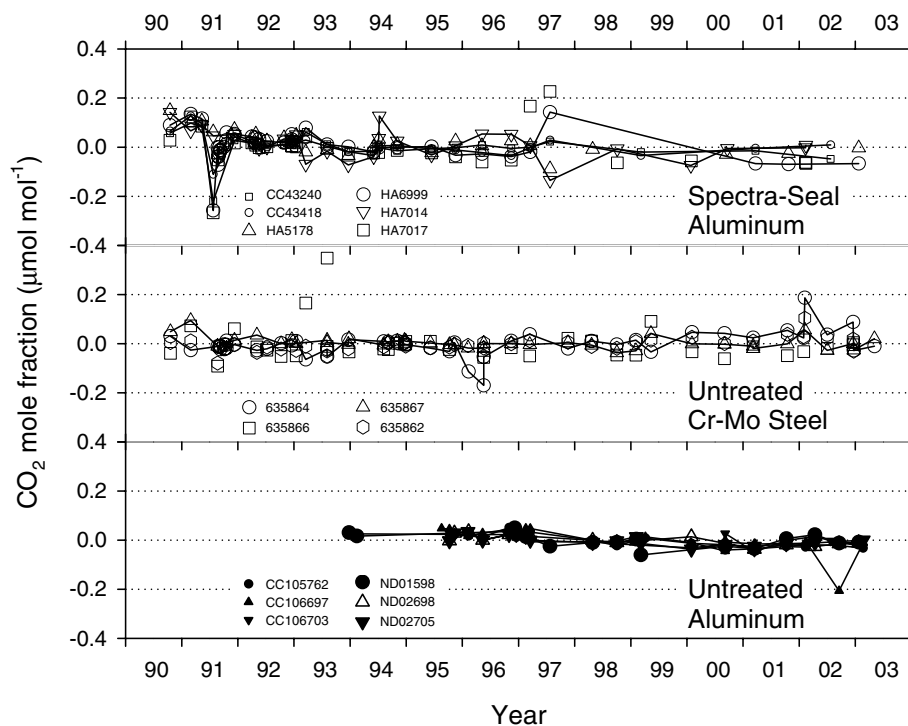


Fig. 4. The same as Fig. 1, except showing  $\text{CO}_2$  concentrations of primary reference tanks.

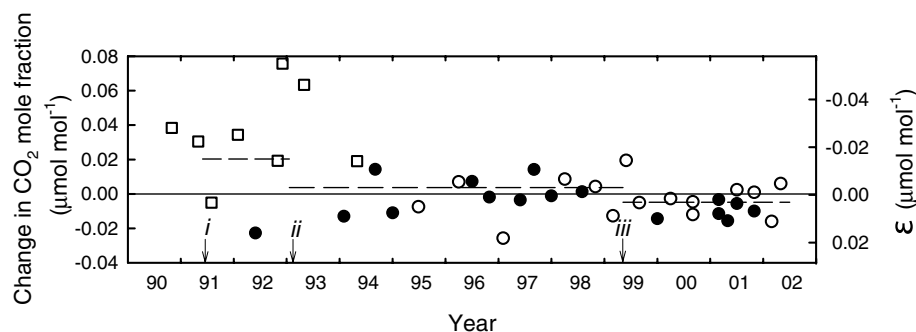


Fig. 5. The same as Fig. 3, except showing the change in the  $\text{CO}_2$  concentration of working tanks between the full tank and the tank with 25% remaining.

combination of gravimetric and thermal fractionation, given that  $\text{CO}_2$  has a higher molecular weight than  $\text{O}_2$  and  $\text{N}_2$ , and so should tend to accumulate over time in the tank.

In contrast to the experiences of other laboratories, we find little tendency of  $\text{CO}_2$  to drift upwards with usage. As shown in Fig. 5, the drift experienced by our working tanks has been typically much smaller than  $0.05 \mu\text{mol mol}^{-1}$ , and except for steel tanks which probably suffer from stronger surface effects, the drift is consistently within  $\pm 0.02 \mu\text{mol mol}^{-1}$ , corresponding to  $\epsilon$  factors for  $\text{CO}_2$  in the range of  $\pm 0.014 \mu\text{mol mol}^{-1}$ . The implication is that the measures we have taken to reduce thermal fractionation of  $\text{O}_2/\text{N}_2$  have also eliminated the tendency for  $\text{CO}_2$  to drift upwards with tank usage, a result which may be

of some importance to the maintenance of high-stability  $\text{CO}_2$  standards.

The observed bounds on  $\text{CO}_2$  drift are supported by the relative thermal sensitivities of  $\text{CO}_2/\text{N}_2$  and  $\text{O}_2/\text{N}_2$  in air. We have directly measured the relevant ratio  $(\alpha D)_{\text{CO}_2/\text{N}_2}/(\alpha D)_{\text{O}_2/\text{N}_2}$  using the technique described in Keeling et al. (2004), which yielded figures of  $2.9 \pm 0.1$  and  $4.9 \pm 0.2$  at 1 and 120 atm (both at  $20^\circ\text{C}$ ), respectively. Multiplying these dimensionless figures by a typical  $\text{CO}_2$  mole fraction of  $3.6 \times 10^{-4}$  yields relative sensitivities of  $1.1 \pm 0.1 \times 10^{-3} (\mu\text{mol mol}^{-1}) (\text{per meg})^{-1}$  and  $1.8 \pm 0.1 \times 10^{-3} (\mu\text{mol mol}^{-1}) (\text{per meg})^{-1}$  at 1 and 120 atm (both at  $20^\circ\text{C}$ ), respectively. These results suggest that the  $\text{CO}_2$  drift with tank usage can be reduced below  $0.02 \mu\text{mol mol}^{-1}$  through

the introduction of measures that reduce  $O_2/N_2$  drift to below 10 per meg, consistent with our experiences.

The  $CO_2$  results also help to clarify the origin of the 1999 shift noted above in Fig. 3 associated with the laboratory relocation. A downward shift can be seen in the average  $CO_2$  drift at this time (Fig. 5), corresponding to a change in  $\varepsilon$  of  $0.006 \pm 0.004 \mu\text{mol mol}^{-1}$ . The ratio of the shift in  $CO_2$  to  $O_2/N_2$  is  $0.0014 \pm 0.008 (\mu\text{mol mol}^{-1}) (\text{per meg})^{-1}$ , which is in good agreement with the thermal ratio, thus supporting the interpretation, also backed by  $Ar/N_2$  data, that the shift was caused by thermal fractionation.

## 7. Summary and discussion

We have presented results for the relative stability of the  $O_2/N_2$  ratio delivered from a suite of 18 high-pressure tanks filled with compressed air over a period of more than a decade. By comparing air delivered from tanks with different material types and size and configuration, we have placed bounds on the magnitude of tank leakage, corrosion effects, or other surface effects on the  $O_2/N_2$  ratios. We have also placed bounds on thermal, gravimetric, and surface desorption effects by examining the stability of our ‘working tanks’ which are depleted relatively rapidly and hence allow us to detect any systematic trends with changing tank pressure, as would be expected for such processes. Corrosion, leakage, and surface desorption effects are shown to be uniformly smaller than  $\pm 3$  per meg per decade.

Thermal fractionation within the tank remains potentially significant, however, in spite of our efforts to minimize this effect by storing tanks horizontally within a thermally insulated enclosure. The thermal fractionation appears to be typically at the level of  $\pm 3$  per meg or smaller, although the variability is clearly not entirely random. For example, a systematic shift of  $\sim 2$  per meg probably occurred in association with moving our laboratory from one building to another due to changes in the thermal environment.

The results emphasize the importance of using strict protocols for delivering gases from tanks, for maintaining a suite of reference tanks of diverse sizes and material types, and of tracking drift in rapidly depleted tanks as a means of assessing fractionation. Our results also particularly emphasize the value of storing tanks horizontally within an insulated enclosure, a procedure which we have shown also seems to help stabilize  $CO_2$  concentrations.

Table 3 summarizes the estimated contributions of the various processes discussed in this paper to uncertainty in our final (S2)  $O_2/N_2$  calibration scale. The table also illustrates how the results can be combined to estimate the probable bounds on scale drift over various periods. For example, from 1990 to 2000, the estimated bounds are  $\pm 6$  per meg, while from 1992 to 2002, the bounds are  $\pm 4$  per meg. If instability of our scale were the only contribution to uncertainty, these bounds would allow resolving the average changes in land carbon storage to the level

Table 3. Estimated uncertainties in S2 scale

Process	Uncertainty
Corrosion	$\pm 0.3$ per meg $\text{yr}^{-1}$
Leakage & permeation	$\pm 0.2$ per meg $\text{yr}^{-1}$
Thermal fractionation after 7/92	$\pm 2$ per meg
Thermal fractionation before 7/92	$\pm 4$ per meg
Desorption effects	$\pm 0.1$ per meg $\text{yr}^{-1}$
Overall 1990–2000 uncertainty	$\pm 6$ per meg
Overall 1993–2003 uncertainty	$\pm 4$ per meg

of  $\pm 0.24 \text{ Pg C yr}^{-1}$  from 1990 to 2000 and  $\pm 0.16 \text{ Pg C yr}^{-1}$  from 1993 to 2003. These errors are relatively small compared to other errors in the  $O_2$ -based carbon budget, such as uncertainty in fossil-fuel burning and oceanic  $O_2$  outgassing (Manning et al. (2006)).

Several caveats apply to these conclusions. First, the estimated bounds on tank stability depend partly on subjective probability assessments, an example being our assumptions about matching of corrosion rates in different types of tanks. Secondly, the bounds apply only to the specific set of processes identified here. That additional ‘unknown’ processes may be relevant is illustrated, for example, by the short-term scatter in the tank data (as in Figs. 1 and 3), much of which remains unexplained. Whether such additional processes could contribute to parallel drift in the reference gases is unclear. Thirdly, experimental artefacts can also be introduced at the point of collecting samples in the field, during storage of samples in flasks, and during the process of comparing air samples to reference gases (Keeling et al., 1998a). Comparisons between  $O_2/N_2$  data from overlapping stations in the Scripps and Princeton University  $O_2/N_2$  flask networks have revealed systematic shifts that are probably not caused by drifts in calibration gases in either laboratory, and hence may be due to time-varying artefacts at other points in the handling of samples or reference gases.

Several areas needing further work can be identified. First, in spite of the progress made using relative standards to calibrate  $O_2/N_2$  measurements, as documented here, a clear need still exists for developing absolute  $O_2/N_2$  standards or absolute analysis methods. Absolute standards of sufficient accuracy would help overcome any residual uncertainties associated with leakage, corrosion, and other surface effects, and would address any lingering concerns regarding unknown processes. Also, absolute calibration is needed to ensure that measurements of  $O_2/N_2$  ratio made today can be linked with measurements made in the future, beyond the lifespan of the current measurement programmes. Recently, standards were prepared using a gravimetric approach, achieving a precision of  $\sim 16$  per meg on individual standards (Tohjima et al., 2005), which is significantly more precise than that which was achieved previously (Machta and Hughes, 1970). Secondly, an improved understanding is needed of the relevant

high-pressure fractionation processes, such as thermal diffusion at the tank outlet. Measurements are largely lacking, for example, of the diffusivities and thermal diffusivities of the major components of air at high pressures.

## 8. Acknowledgments

We acknowledge useful discussions with Britt Stephens and additional support from Tegan Blaine, Elizabeth McEvoy, Laura Katz, Kim Bracchi, and Tim Lueker. Two anonymous reviewers offered helpful suggestions. This work was supported by the National Science Foundation (NSF) under ATM-872037, ATM-9309765, ATM-9612518, ATM-0000923 and ATM03-30096, by the Environmental Protection Agency (EPA) under IAG#DW49935603- 01-2, and by the National Oceanic and Atmospheric Administration (NOAA) under NA77RJ0453A. Any opinions, findings and conclusions or recommendations expressed in this material are those of the authors and do not necessarily reflect the views of NSF, EPA or NOAA.

## References

- Balkanski, Y., Monfray, P., Battle, M. and Heimann, M. 1999. Ocean primary production derived from satellite data: An evaluation with atmospheric oxygen measurements. *Glob. Biogeochem. Cycle* **13**, 257–271.
- Battle, M., Bender, M. L., Tans, P. P., White, J. W. C., Ellis, J. T. and co-authors. 2000. Global carbon sinks and their variability inferred from atmospheric O<sub>2</sub> and  $\delta^{13}\text{C}$ . *Science* **287**, 2467–2470.
- Bender, M. L., Tans, P. P., Ellis, J. T., Orchardo, J. and Habfast, K. 1994. A high-precision isotope ratio mass-spectrometry method for measuring the O<sub>2</sub>/N<sub>2</sub> ratio of air. *Geochim. Cosmochim. Acta* **58**, 4751–4758.
- Bender, M. L., Ho, D. T., Hendricks, M. B., Mika, R., Battle, M. O. and co-authors. 2005. Atmospheric O<sub>2</sub>/N<sub>2</sub> changes, 1993–2002: Implications for the partitioning of fossil fuel CO<sub>2</sub> sequestration. *Glob. Biogeochem. Cycle* **19**(GB4017), 4011–4015.
- Broecker, W. S. 1970. Man's oxygen reserves. *Science* **168**, 1537–1538.
- Keeling, R. F. 1988a. Measuring correlations between atmospheric oxygen and carbon-dioxide mole fractions - a preliminary study in urban air. *J. Atmos. Chem.* **7**, 153–176.
- Keeling, R. F. 1988b. *Development of an Interferometric Oxygen Analyzer for Precise Measurement of the Atmospheric O<sub>2</sub> Mole Fraction*. Harvard University, 178.
- Keeling, R. F. and Shertz, S. R. 1992. Seasonal and interannual variations in atmospheric oxygen and implications for the global carbon-cycle. *Nature* **358**, 723–727.
- Keeling, R. F., Najjar, R. P., Bender, M. L. and Tans, P. P. 1993. What atmospheric oxygen measurements can tell us about the global carbon-cycle. *Glob. Biogeochem. Cycle* **7**, 37–67.
- Keeling, R. F., Piper, S. C. and Heimann, M. 1996. Global and hemispheric CO<sub>2</sub> sinks deduced from changes in atmospheric O<sub>2</sub> concentration. *Nature* **381**, 218–221.
- Keeling, R. F., Manning, A. C., McEvoy, E. M. and Shertz, S. R. 1998a. Methods for measuring changes in atmospheric O<sub>2</sub> concentration and their application in southern hemisphere air. *J. Geophys. Res.-Atmos.* **103**, 3381–3397.
- Keeling, R. F., Stephens, B. B., Najjar, R. G., Doney, S. C., Archer, D. and co-authors. 1998b. Seasonal variations in the atmospheric O<sub>2</sub>/N<sub>2</sub> ratio in relation to the kinetics of air-sea gas exchange. *Glob. Biogeochem. Cycle* **12**, 141–163.
- Keeling, R. F., Blaine, T., Paplawsky, B., Katz, L., Atwood, C. and co-authors. 2004. Measurement of changes in atmospheric Ar/N<sub>2</sub> ratio using a rapid-switching, single-capillary mass spectrometer system. *Tellus* **56B**, 322–338.
- Langenfelds, R. L. 2002. Studies of the carbon cycle using atmospheric oxygen and associated tracers. University of Tasmania, 338.
- Machta, L. and Hughes, E. 1970. Atmospheric Oxygen in 1967 to 1970. *Science* **168**, 1582–1584.
- Manning, A. C., Keeling, R. F. and Severinghaus, J. P. 1999. Precise atmospheric oxygen measurements with a paramagnetic oxygen analyzer. *Glob. Biogeochem. Cycle* **13**, 1107–1115.
- Manning, A. C. and Keeling, R. F. 2006. Global oceanic and land biotic carbon sinks from the Scripps atmospheric oxygen flask sampling network. *Tellus* **58B**, 95–116.
- Najjar, R. G. and Keeling, R. F. 2000. Mean annual cycle of the air-sea oxygen flux: A global view. *Glob. Biogeochem. Cycle* **14**, 573–584.
- Reid, R. C., Prausnitz, J. M. and Poling, B. E. 1987. *The Properties of Gases and Liquids* 4th Edition. McGraw-Hill, New York.
- Stephens, B. B., Keeling, R. F., Heimann, M., Six, K. D., Murnane, R. and co-authors. 1998. Testing global ocean carbon cycle models using measurements of atmospheric O<sub>2</sub> and CO<sub>2</sub> concentration. *Glob. Biogeochem. Cycle* **12**, 213–230.
- Stephens, B. B., Keeling, R. F. and Paplawsky, W. 2003. Shipboard measurements of atmospheric oxygen using a vacuum-ultraviolet absorption technique. *Tellus* **55B**, 857–878.
- Stephens, B. B., Bakwin, P., Tans, P. P., Teclaw, R. and Baumann, D. 2006. Application of a differential fuel-cell analyzer for measuring atmospheric oxygen variations. *Journal of atmospheric and oceanic technology* in press.
- Sturm, P., Leuenberger, M., Sirignano, C., Neubert, R. E. M., Meijer, H. A. J. and co-authors. 2004. Permeation of atmospheric gases through polymer O-rings used in flasks for air sampling. *J. Geophys. Res.-Atmos.* **109**, D04309.
- Tohjima, Y. 2000. Method for measuring changes in the atmospheric O<sub>2</sub>/N<sub>2</sub> ratio by a gas chromatograph equipped with a thermal conductivity detector. *J. Geophys. Res.-Atmos.* **105**, 14575–14584.
- Tohjima, Y., Machida, T., Watai, T., Akama, I., Amari, T. and co-authors. 2005. Preparation of gravimetric standards for measurements of atmospheric oxygen and reevaluation of atmospheric oxygen concentration. *J. Geophys. Res.-Atmos.* **110**, D11302.